Earth's Future

RESEARCH ARTICLE
10.1029/2023EF004292

Anomalous Water Vapor Circulation in an Extreme Drought Event of the Mid-Reaches of the Lancang-Mekong River Basin

Guoqing Gong[1], Shuyu Zhang[1], Baoni Li[1], Yufan Chen[1], Penghan Chen[1], Kai Wang[1], Thian Yew Gan[2,3], Deliang Chen[4], and Junguo Liu[1,5]

[1]School of Environmental Science and Engineering, Southern University of Science and Technology, Shenzhen, China, [2]Department of Civil and Environmental Engineering, University of Alberta, Edmonton, AB, Canada, [3]Department of Environmental Studies, University of Colorado at Boulder, Boulder, CO, USA, [4]Department of Earth Sciences, University of Gothenburg, Gothenburg, Sweden, [5]Henan Provincial Key Laboratory of Hydrosphere and Watershed Water Security, North China University of Water Resources and Electric Power, Zhengzhou, China

Abstract The middle reaches of the Lancang-Mekong River Basin (M-LMRB) experienced a record-breaking drought event in 2019, resulting in significant economic losses of approximately 650 million dollars and affecting a population of 17 million. However, the anomalous circulation and transportation processes of water vapor, which may have played a crucial role in inducing the extreme drought, have not been fully studied. In this study, we analyze the water vapor circulation during the 2019 drought event using the land-atmosphere water balance and a backward trajectory model for moisture tracking. Our results indicate that the precipitation in the M-LMRB from May to October 2019 was only 71.9% of the long-term climatological mean (1959–2021). The low precipitation during this drought event can be attributed to less-than-normal external water vapor supply. Specifically, the backward trajectory model reveals a decrease in the amount of water vapor transported from the Indian Ocean, the Bay of Bengal, and the Pacific Ocean, which are the main moisture sources for precipitation in the region. Comparing the atmospheric circulation patterns in 2019 with the climatology, we identify anomalous anticyclone conditions in the Bay of Bengal, anomalous westerlies in the Northeast Indian Ocean, and an anomalous cyclone in the Western Pacific Ocean, collectively facilitating a stronger export of water vapor from the region. Therefore, the dynamic processes played a more significant role than thermodynamic processes in contributing to the 2019 extreme drought event.

Plain Language Summary In 2019, a record-breaking drought hit the M-LMRB, leading to significant economic losses and affecting a large population. This study explores the water vapor circulation during this drought using land-atmosphere water balance and a backward trajectory model. Findings show that precipitation from May to October 2019 was only seventy percent of the average from 1959 to 2021. The drought's severity was mainly due to a lack of water vapor from key sources: the Indian Ocean, the Bay of Bengal, and the Pacific Ocean. Anomalous weather patterns—an anticyclone in the Bay of Bengal, unusual westerlies in the Northeast Indian Ocean, and a cyclone in the Western Pacific—led to a significant reduction in water vapor reaching the region. This indicates that dynamic atmospheric processes played a larger role in causing the extreme drought than thermodynamic ones. These insights help improve understanding and prediction of droughts in Southeast Asia, particularly under changing climate conditions.

Guoqing Gong and Shuyu Zhang contributed equally to this work.

Key Points:

- Reduced external water vapor transport primarily leads to negative precipitation anomalies
- There has been a reduction in water vapor originating from the Indian Ocean, Bay of Bengal, and Pacific Ocean
- The reduction in water vapor transport is primarily influenced by dynamic factors rather than thermodynamic ones

Supporting Information:

Supporting Information may be found in the online version of this article.

Correspondence to:

J. Liu,
junguo.liu@gmail.com

Citation:

Gong, G., Zhang, S., Li, B., Chen, Y., Chen, P., Wang, K., et al. (2024). Anomalous water vapor circulation in an extreme drought event of the mid-reaches of the Lancang-Mekong River basin. *Earth's Future*, *12*, e2023EF004292. https://doi.org/10.1029/2023EF004292

Received 3 DEC 2023
Accepted 16 JUL 2024

1. Introduction

Drought is one of the most devastating natural hazards that has killed about 650,000 people across the world over the last 50 years and resulted in 124 billion US dollars of economic losses over the past 20 years (Daniel et al., 2022). Under the impact of climate warming, the frequency and intensity of drought occurrences is increasing and has spread beyond traditional arid and semi-arid regions (Ault, 2020; Chiang et al., 2021; Daniel et al., 2022; Z. Li et al., 2024; Parmesan et al., 2022; Xiong et al., 2022; Yang et al., 2019). The severe droughts of northeastern Brazil from 2012 to 2016 resulted in about 30 billion US dollars in economic losses and affected a population of 33.4 million (de Medeiros et al., 2020; Marengo et al., 2017). In Europe, crop losses due to droughts have tripled over the past 50 years, which has threatened the regional and global agricultural security (Brás et al., 2021; Markonis et al., 2021; van der Wiel et al., 2023). In recent decades, the Lancang-Mekong River Basin

(LMRB) has also experienced more frequent and intensive droughts, especially during the wet season (May to October) (Mekong River Commission, 2021).

As the longest river in Southeast Asia (Gupta et al., 2002), flowing through six countries, namely China, Myanmar, Thailand, Laos, Cambodia and Vietnam, Lancang-Mekong River provides fresh water for approximately 70 million residents (Feng et al., 2019). However, the upper and middle reaches of the basin, as well as Thailand, Cambodia and southern Vietnam, have been significantly impacted by these drought events (Tian et al., 2020). In 1998, Vietnam experienced a widespread drought, resulting in estimated agricultural production losses exceeding $400 million (Nguyen & Shaw, 2011a). Similarly, in 2002, Cambodia faced a similar drought, which devastated 100,000 ha of rice fields (Nguyen & Shaw, 2011b). Over a decade later, the drought of 2016 inflicted significant economic losses on Thailand ($1.7 billion) and affected over 9.56 million people (Mekong River Commission, 2021). According to climate projections by global climate models, the intensity and frequency of future droughts in the LMRB will increase consistently with global warming (Dong et al., 2022).

The formation of drought is generally associated with a rapid decrease in precipitation over a period, which further leads to an increase in atmospheric evaporative demand, a reduction in soil moisture, and a decrease in runoff (Bevacqua et al., 2022; Gu et al., 2020; Wang et al., 2023). Recent studies have contributed to our understanding of the drought mechanisms associated with decreased precipitation. For example, the increase in drought frequency in Cape Town is primarily attributed to the expansion of the Hadley circulation toward the poles and the associated southward shift in storm tracks (Burls et al., 2019). The long-term drought trend in Central Equatorial Africa over the last 20 years was possibly because of the westward expansion of the Walker circulation and reduced low-level moisture transport (Barichivich et al., 2018). In 2019, the LMRB experienced the worst drought in the past century (Lu & Chua, 2021), causing economic losses of about 650 million US dollars and affecting the livelihoods of 17 million residents of 13 provinces in the Mekong Delta area (Mekong River Commission, 2022). Studies have shown that a strong El Niño event was the main cause of this mega-drought, leading to the delayed arrival and early withdrawal of the monsoons, mainly by modulating the tropical Walker circulation and also by weakening the monsoons with the superposition of positive Indian Ocean Dipoles (Indian Meteorological Department, 2020; Mekong River Commission, 2021; Ratna et al., 2021; Wang et al., 2020). Moreover, anomalously high temperatures with strong El Niño events enhanced the evapotranspiration process, which further aggravated the drought hazard (Sam et al., 2019).

Even though teleconnections between the 2019 drought and large-scale climate patterns have been analyzed thoroughly (M. H. Li et al., 2023; X. Li et al., 2023; Phan-Van et al., 2022), there is still limited understanding of the anomalies in water vapor flux and moisture supply, which are crucial for precipitation formation. It is essential to identify the water vapor circulation processes and quantify the contributions from different moisture sources to better comprehend and predict drought events in the LMRB.

Moisture associated with the precipitation of a specific region is usually transported from external sources and recirculated from the local evapotranspiration. Precipitation recirculation rate (PRR), defined as the proportion of precipitation caused by local evapotranspiration over the total precipitation, could be used to evaluate the circulation of water vapor in a specific region (Eltahir & Bras, 1994, 1996; Sui et al., 2007). To estimate the PRR for the Loess Plateau, the Brubaker model (Brubaker et al., 1993; Zhao & Zhou, 2021) has been used to consider mixing processes of the water vapor movement, Tian et al. (2022) found an increase in the PRR from 9.16% to 10.18% after the region has undergone large-scale afforestation. During the extreme drought of 2019, PRR at the middle and lower reaches of the Yangtze River had increased by 8.4% mainly due to a significant reduction of external water vapor fluxes (Guan et al., 2022). For external moisture transport, backward trajectory tracking is usually used to identify water vapor pathways and sources. The Hybrid Single-Particle Lagrangian Integrated Trajectory (HYSPLIT) model is one of the most widely used models to quantify the air parcel trajectories and sources backward (Stein et al., 2015). It has been used to assess the moisture sources and pathways associated with drought onset and termination in the monsoon region (Shah & Mishra, 2020).

Zhao and Zhou (2021) conducted an evaluation of various methods for calculating the PRR, acknowledging that the Brubaker model relies on certain assumptions such as the uniformity of surface features, which may not be fully applicable in real-world scenarios. However, despite these limitations, the study recommended the Brubaker model as the most suitable algorithm. This endorsement stems from the model's comprehensive consideration of moisture mixing processes (Guan et al., 2022), which ultimately reduces uncertainties associated with PRR calculations. In the case of HYSPLIT, as a Lagrangian-based water vapor tracking method (Shi et al., 2020; Stein

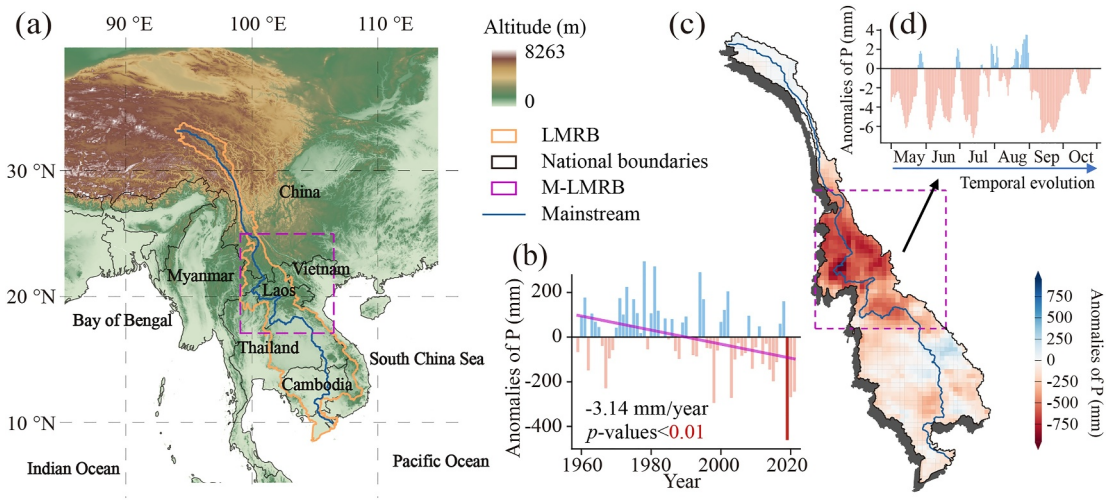

Figure 1. (a) Topography of the LMRB highlighting the study area, M-LMRB, in a purple rectangle; (b) Time series of precipitation anomalies in the M-LMRB (1959–2021), with blue bars indicating positive anomalies, red bars indicating negative anomalies, and 2019 highlighted in dark red. The trend and significance were detected through linear regression; (c) Spatial distribution of precipitation anomalies during the 2019 wet season (May to October) compared to the long-term mean of wet seasons from 1959 to 2021 in the M-LMRB; (d) Weekly moving average of precipitation anomalies in the M-LMRB during the wet season of 2019.

et al., 2015), simulating complex atmospheric dynamics typically demands significant computational resources (Dey & Döös, 2020). Compared to isotope tracking methods, the HYSPLIT model directly reveals transport trajectories, providing an intuitive representation of the transport process from source to sink, thereby facilitating a deeper understanding of atmospheric transport processes (Diekmann et al., 2021; Yuan et al., 2020).

Therefore, we employed the Brubaker model and HYSPLIT model to investigate the roles of moisture cycling, sources, and transport in the unprecedented drought of the LMRB in 2019. Our objective is to address the following questions to fill the knowledge gap regarding water supply during this extreme drought event: During this drought period, what were the contributions of remote moisture transport and regional evapotranspiration dynamics to moisture patterns? Which moisture origins and transport mechanisms were influential in the occurrence of extreme drought events? Were the deviations in moisture transport primarily driven by dynamic or thermodynamic processes? The remainder of this article is organized as follows: Section 2 provides a comprehensive description of the study area, including details on data collection and the methods employed in our research; Section 3 discusses the results, highlights the key findings and outcomes; Results are discussed and summarized in Section 4 to provide a thorough interpretation of the main findings.

2. Data and Methods

2.1. Study Area

As the LMRB is situated in Southeast Asia, its precipitation is affected by the Asian monsoon system (Wang et al., 2022). The long-term (1959–2021) annual precipitation of LMRB is 1,691 mm but with large spatial variations, such that precipitation is higher in the southeast and lower in the northwest (Liu et al., 2022). The focus of this study is on the mid-reaches of LMRB (M-LMRB) (Figure 1a), which had experienced significant precipitation anomalies in 2019 (Figure 1c). The M-LMRB accounts for approximately 36.1% of the total area of the LMRB and contributes to 41.8% of its total precipitation. The agricultural sector in the southern part of the M-LMRB heavily relies on precipitation for crop growth and productivity (Tang et al., 2021). In addition, the altitude of the study area varies widely, ranging from 78 m in the southeast to 3,259 m in the northwest. Due to large elevation differences and high water demand, in recent years multiple dams have been built in China, Laos, and Myanmar for water storage, aquaculture and power generation, respectively (Yun et al., 2021).

The 2019 wet season precipitation in M-LMRB was 1,178 mm, which was much lower than its long-term mean of 1,639 mm (Figure 1b). Examining the temporal evolution of precipitation, almost the entire 2019 wet season exhibited negative anomalies in precipitation, with only a few instances of positive anomalies providing some relief from drought (Figure 1d). Spatially, the anomalous precipitation was much lower in the northern region of

M-LMRB which suffered more severe drought than the southern region (Figure 1c), particularly at the junction between China, Laos and Myanmar, where the negative precipitation anomaly was as high as 750 mm, which severely affected the agricultural production and residents' living, even causing regional conflicts (Lu et al., 2021).

2.2. Hydrometeorological Data

The sparsity and uneven distribution of measurement stations pose challenges to the monitoring of meteorological variables in the LMRB. Prior research has underscored the applicability of the Asian Precipitation-Highly Resolved Observational Data Integration Toward Evaluation (APHRODITE) (Irannezhad et al., 2022) and the Global Precipitation Climatology Centre (GPCC) data sets (Irannezhad et al., 2020) for the LMRB. Nonetheless, these data sets do not include data from the year 2019. Given the high spatial resolution ($0.25° \times 0.25°$) and longer record period (1940-present) of ERA5 (ECMWF Reanalysis fifth) reanalysis data set (Hersbach et al., 2020), provide representative convective rainfall and water vapor convergence patterns (Mahto & Mishra, 2019; Nogueira, 2020), and have been previously employed in related studies on annual maximum precipitation in the LMRB (Zhang et al., 2024). Additionally, compared to other reanalysis data sets such as MERRA-2, ERA5 reanalysis data exhibit lower uncertainty in assessing wind speed and water vapor transport (Gualtieri, 2022; Olauson, 2018). Therefore, this study obtained hourly ERA5 data including zonal and meridional winds (m/s), specific humidity (kg/kg), precipitation (mm), evapotranspiration (mm), runoff (mm), 2-m temperature (°C), vertically integrated water vapor divergence (kg/(m^2·s)), northward vertical integrated moisture flux (kg/(m·s)), and eastward vertical integrated moisture flux (kg/(m·s)) from 1959 to 2021 during the wet season (May to October), and aggregated them into daily data.

The NCEP/NCAR Reanalysis 1 data set (NCEP/NCAR-R1) (Kalnay et al., 2018) is widely used and has a long record, covering the period from 1948 to the present. The NCEP/NCAR-R1 has frequently served as the primary meteorological input for HYSPLIT dispersion modeling in prior research, often chosen over alternative data sets for its established reliability and compatibility with atmospheric dispersion studies (Guo et al., 2023; Liu et al., 2023). Additionally, NCEP/NCAR-R1 has been widely used for moisture tracking analysis in the LMRB (Zhang et al., 2024) and other Asian monsoon regions (Guan et al., 2022; Suthinkumar et al., 2023). Therefore, for this analysis, six-hourly data of air temperature (°C), meridional and zonal winds (m/s), vertical velocity (Pa/s), and specific humidity (kg/kg) were extracted from the NCEP/NCAR-R1 data set. These variables were obtained at 17 pressure levels, ranging from 1,000 to 10 hPa, to capture the vertical structure of the atmosphere. The data covered the wet seasons of the years 1959–2021, allowing for a comprehensive assessment of moisture transport patterns and pathways during this period.

2.3. Methods

In this study, the Brubaker model was used to analyze the PRR for quantifying the contribution of local evapotranspiration and external water vapor fluxes to precipitation. We aim to determine the extent to which local evapotranspiration and external water vapor fluxes influence precipitation patterns in the area, but it is challenging to quantify the specific external effect. Therefore, the HYSPLIT model was used to identify the possible source and pathway of the water vapor transport that contributes to the precipitation of the middle region of LMRB. According to the water vapor flux equation, changes in atmospheric circulation and temperature both contribute to the development of precipitation anomalies (Kumari et al., 2022; Tan et al., 2019; Wang et al., 2021). Therefore, the dynamic (wind) and thermodynamic (temperature) contributions affecting water vapor transport are quantified.

2.3.1. Precipitation Recycling Ratio and Moisture Transport Decomposition

The two-dimensional method for estimating PRR developed by Brubaker et al. (1993) was utilized. The PRR is estimated based on three assumptions: (a) Sufficient time: a long and continuous time period is required to ensure that the externally transported and locally evaporated water vapor are well mixed; (b) Negligible vertical moisture flux: The vertical moisture flux is considered negligible compared to the horizontal moisture flux (Burde & Zangvil, 2001), allowing the focus to be on the horizontal movement and exchange of moisture; (c) Equal proportions of evaporative and advected moisture: It is assumed that the proportion of evaporative and advective water vapor is equal in both precipitation and moisture flux across different time periods.

The feasibility of using the PRR method has been confirmed in the Asian monsoon region (Guan et al., 2022). For this study, a 6-month time period from May to October was selected, meeting the prerequisites for moisture mixing.

In the context of a land region, the water balance equation can be expressed as:

$$R + \Delta SM = P - E \tag{1}$$

where R represents runoff (mm), ΔSM denotes the change of land moisture storage (mm), P and E represents precipitation (mm) and evapotranspiration (mm) respectively. This equation describes the regional water balance.

The water vapor flux data is obtained directly from the ERA5 data set, which represents the water vapor flux integral from the land surface (1,000 hPa) to the top of the atmosphere (10 hPa) based on the following equation:

$$Q = \frac{1}{g}\int_{p_{surf}}^{p_{top}} qVdp \tag{2}$$

where, Q represents the total column water vapor (kg/(m·s)), g is acceleration of gravity ((Pa·m^2)/kg), q is the specific humidity (g/kg), V is the horizontal wind (m/s), p_{surf} and p_{top} (hPa) are the atmospheric pressure at the surface and at the top of atmosphere, respectively. The change of atmospheric humidity can be expressed as:

$$\frac{\partial F}{\partial t} = -\left(\frac{\partial F_u}{\partial x} + \frac{\partial F_v}{\partial y}\right) + E - P \tag{3}$$

In the right side of Equation 3, $-\left(\frac{\partial F_u}{\partial x} + \frac{\partial F_v}{\partial y}\right)$ is the horizontal moisture flux dispersion (mm/m^2), E is the average evapotranspiration per unit area (mm/m^2), and P is the average precipitation per unit area (mm/m^2). For each square meter of the air column, the variation of vertical moisture flux dispersion over time $\frac{\partial F}{\partial t}$ can be represented by Equation 3. According to the second assumption, the vertical variation of moisture flux dispersion is negligible compared to the horizontal variation over a long time period, then $\frac{\partial F}{\partial t} \approx 0$. Therefore, the atmospheric moisture budget in the unit area was made:

$$P = -\left(\frac{\partial F_u}{\partial x} + \frac{\partial F_v}{\partial y}\right) + E \tag{4}$$

Similar to Equation 4, the precipitation originated from external moisture advection (P_a) per unit area is written as:

$$P_a = -\left(\frac{\partial F_u^a}{\partial x} + \frac{\partial F_v^a}{\partial y}\right) \tag{5}$$

where the terms on the right side are the convergence of the external advected moisture. Using Equations 4 and 5, the following equations can be applied in the study region (A):

$$-\left(\frac{\partial F_u}{\partial x} + \frac{\partial F_v}{\partial y}\right)|A = F_{in} - F_{out} = (P - E)A \tag{6}$$

$$-\left(\frac{\partial F_u^a}{\partial x} + \frac{\partial F_v^a}{\partial y}\right)|A = F_{in} - F_{out-a} = P_a A \tag{7}$$

where, A is the area of the region, F_{in} and F_{out} are the inflow and outflow of the atmospheric moisture, respectively. $F_{out\text{-}a}$ is the outflow of the external advected moisture. As shown in Equations 6 and 7, F_{out} and $F_{out\text{-}a}$ are positively related with F_{in} (Zhao & Zhou, 2021), so the mean moisture flux in the atmosphere can be represented as the arithmetic average of the inflow and outflow:

$$\overline{F} = \frac{F_{in} + F_{out}}{2} = F_{in} - \frac{(P - E)A}{2} \tag{8}$$

$$\overline{F}_a = \frac{F_{in} + F_{out-a}}{2} = F_{in} - \frac{P_a A}{2} \tag{9}$$

According to the third assumption, the proportions of the evaporative and advected moisture are equal in both precipitation and atmospheric moisture:

$$\frac{P_a}{P} = \frac{F_a}{\overline{F}} \tag{10}$$

Applying Equations 9 and 10 to Equation 11, the contribution of external advected moisture to the precipitation can be derived as:

$$\frac{P_a}{P} = \frac{2F_{in}}{2F_{in} + EA} \tag{11}$$

According to the definition of PRR, which can be expressed as:

$$\rho = \frac{P - P_a}{P} \tag{12}$$

where, ρ represents the PRR (%) and P_a is the precipitation from local evapotranspiration.

Therefore, the PRR is obtained as:

$$\rho = \frac{EA}{2F_{in} + EA} \tag{13}$$

where, EA is the regionally averaged evapotranspiration (kg/(m·s)), F_{in} is the vertically integrated water vapor transported into the study area (kg/(m·s)). More details of the Brubaker PRR method can be found in Brubaker et al. (1993).

To analyze the contributions of thermodynamic and dynamic processes to water vapor transport and precipitation, Seager et al. (2010) proposed a method that separates the effects of wind speed (V) and specific humidity (q) on total water vapor transport.

In this study, the pressure level of 300 hPa was selected as the top atmosphere because the atmospheric moisture content above this level is considered negligible (Sun & Lindzen, 1993). Thus, Equation 2 can be decomposed as follows:

$$\begin{aligned}\frac{1}{g}\int_{p_{1000}}^{p_{300}} qV dp &= \frac{1}{g}\int_{p_{1000}}^{p_{300}} (q_c + q_a)(V_c + V_a)\, dp \\ &= \frac{1}{g}\int_{p_{1000}}^{p_{300}} q_c V_c dp + \frac{1}{g}\int_{p_{1000}}^{p_{300}} q_c V_a dp + \frac{1}{g}\int_{p_{1000}}^{p_{300}} q_a V_c dp + \frac{1}{g}\int_{p_{1000}}^{p_{300}} q_a V_a dp\end{aligned} \tag{14}$$

The V and q for a given period can be expressed as $V = V_c + V_a$, $q = q_a + q_c$. In this study, V_c and q_c are the long-term means of wind speed and specific humidity during 1959–2021, respectively, while V_a and q_a are the anomalies of V and q, respectively. In Equation 14, $\frac{1}{g}\int_{p_{1000}}^{p_{300}} q_c V_c dp$ is, therefore, a constant, and $\frac{1}{g}\int_{p_{1000}}^{p_{300}} q_a V_a dp$ can be neglected due to the small deviations of both q_a and V_a relative to the long-term means. Therefore, contributions from dynamics and thermodynamics to the changes in water vapor transport could be quantified by $\frac{1}{g}\int_{p_{1000}}^{p_{300}} q_c V_a dp$ and $\frac{1}{g}\int_{p_{1000}}^{p_{300}} q_a V_c dp$.

2.3.2. Moisture Transport and Trajectories Clustering

The HYSPLIT model, developed by NOAA's Air Resources Laboratory (ARL) (Draxler & Hess, 1998), is widely used to compute air parcel trajectories and particle transport, dispersion, chemical transformation, and deposition simulations (Stein et al., 2015). The model is based on the Lagrangian algorithm, which tracks the movement of air parcels and calculates their moisture changes over a given time interval. The moisture change of an air parcel within a time step is determined by the difference between its evapotranspiration and precipitation amounts.

$$E - P = m\frac{\Delta q}{\Delta t} \tag{15}$$

where m is the air mass (kg/m^2), $\frac{\Delta q}{\Delta t}$ is the change of specific humidity within a time step (1-hr in this study), a negative value of specific humidity ($\frac{\Delta q}{\Delta t} < 0$) indicates moisture release and form precipitation (Sodemann et al., 2008). The HYSPLIT model was used to track the source and pathway of moisture over the M-LMRB during the wet seasons of 1959–2021. 27 points in the study area were evenly selected as the initial location for tracking moisture trajectories (Figure S1 in Supporting Information S1), and the source and pathways of moisture in the previous 10 days were tracked at 1-hr intervals. A total of 312,984 trajectories were tracked in the study area and period, of which 87,062 trajectories were effective precipitation for the M-LMRB.

Self-Organized Map (SOM) algorithm was applied to cluster the selected trajectories. SOM is an unsupervised machine learning algorithm that performs a non-linear transformation of data sets with multiple dimensions onto structured two-dimensional grids (Guntu et al., 2020; Horton et al., 2015; Tan et al., 2019). The use of SOM for event classification offers several advantages. One of the primary benefits is that it does not require any pre-requisite assumptions or prior knowledge about the eventual appearance of the map (Guntu et al., 2020; Loikith et al., 2017; Markonis et al., 2021). The analysis of the training data is conducted in an unbiased manner as SOM solely uses values of the training data at various time steps, without relying on any information regarding the trajectory source themselves. Hence, the utilization of SOM for cluster analysis of meteorological data has been extensively adopted (Chang et al., 2010; Liao et al., 2020; Loikith et al., 2017; Spassiani & Mason, 2021). Using the clustering abilities of SOM, we can group together spatial distributions that are similar according to their trajectories. This enables us to analyze which groups behave similarly and identify which regions have similar water vapor supply patterns, so that we can study their behavior in detail. Therefore, effective trajectories were divided into 20 clusters and the sources regions of moisture were divided into five groups according to the moisture source of the 20 clusters: Indian Ocean (IO), Bay of Bengal (BOB), Pacific Ocean (PO), M-LMRB and South China Sea (SCS), and then the contributions of trajectories of atmospheric moisture content from each region were analyzed.

3. Results

3.1. Hydro-Climatological Characteristics of the 2019 Drought in M-LMRB

The 2-m temperature (Ta) anomalies, evapotranspiration (E) anomalies and runoff (R) anomalies of the M-LMRB during the wet seasons from 1959 to 2019 are shown in Figure 2. The anomalies of Ta and E of the M-LMRB both show significant increasing trends. Ta in 2019 was 1.4°C higher than the long-term mean Ta (Figure 2a), while E in 2019 was 7.2 mm (1.2%) less than the long-term mean (Figure 2b). Consequently, runoff decreased by 427.5 mm (a decrease of 50.2%), reaching its lowest value in recent decades. The spatial distribution of Ta in 2019 shows strong warming especially in the north. It was observed that more regions exhibited negative E anomalies compared to those showing positive anomalies, which was likely caused by insufficient land water content (Jing et al., 2020). Runoff exhibited strong negative anomalies across almost the entire M-LMRB, a spatial feature like that of precipitation anomalies. Further analysis of the temporal evolution of Ta, E, and runoff anomalies using weekly moving average revealed that Ta exhibited positive anomalies throughout the wet season, while E showed a fluctuating trend, with several precipitation events leading to positive anomalies in E. Runoff, on the other hand, displayed negative anomalies throughout almost the entire wet season.

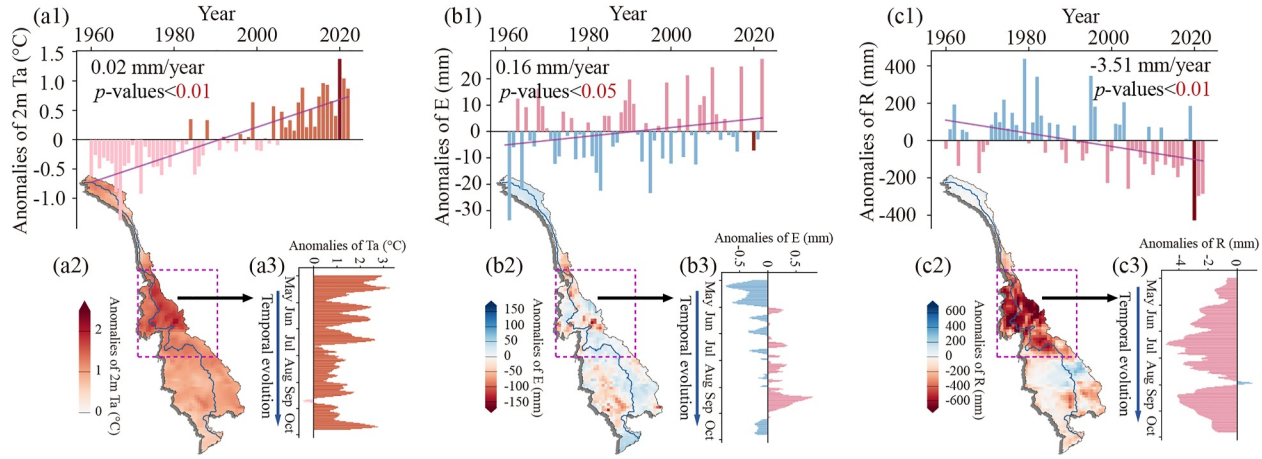

Figure 2. Hydro-meteorological characteristics of the 2019 wet season in M-LMRB: (a1) time series of the M-LMRB averaged 2-m temperature anomalies (1959–2021); (b1) time series of the M-LMRB averaged evapotranspiration anomalies; (c1) time series of the M-LMRB averaged runoff anomalies; (a2) spatial distributions of the 2-m temperature anomalies; (b2) spatial distributions of the evapotranspiration anomalies; (c2) spatial distributions of the runoff anomalies; (a3) Weekly moving average of 2-m temperature anomalies in M-LMRB during the wet season of 2019; (b3) Weekly moving average of evapotranspiration anomalies in M-LMRB during the wet season of 2019; (c3) Weekly moving average of runoff anomalies in M-LMRB during the wet season of 2019. The trend and significance were detected through linear regression; M-LMRB in purple rectangle.

3.2. Precipitation Recycling Ratio (PRR)

The PRR for the extreme drought event in the 2019 wet season and its comparison with the long-term mean are presented in Figure 3. Over the study period, M-LMRB received approximately 2.7 times more precipitation than

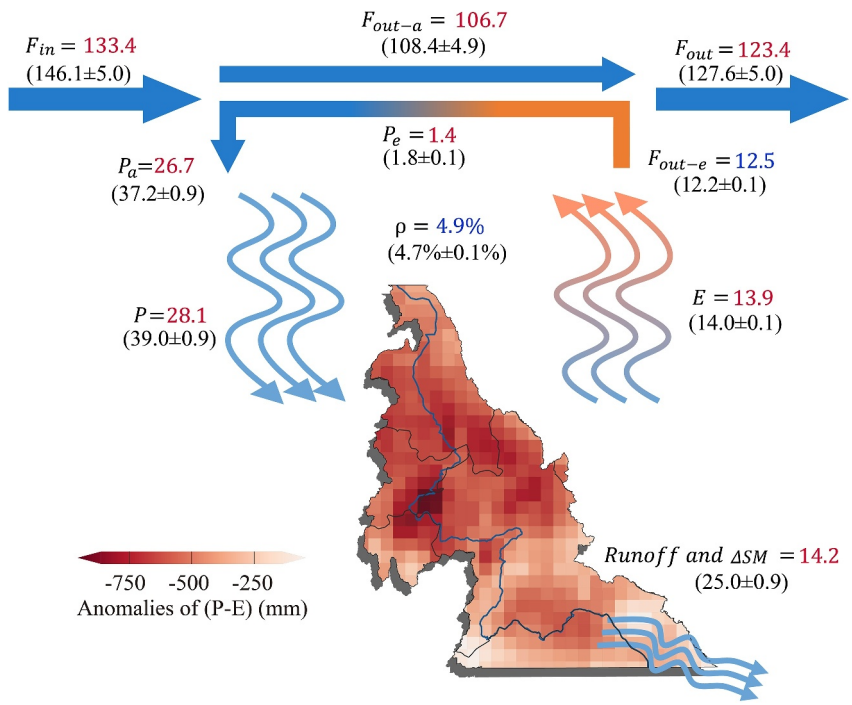

Figure 3. The land-atmosphere water balance for the drought event and the climatological period over the M-LMRB. Definitions of variables (F_{in}, $F_{out\text{-}a}$, $F_{out\text{-}e}$, F_{out}, P_a, P_e, P, E, ρ, *Runoff* and ΔSM) are provided in Section 2.3 (units: 10^6 kg/s). The base map indicates anomalies of ($P - E$). Values in blue and red indicate the positive and negative anomalies during the wet season of 2019, respectively. Values in the parentheses indicate the long-term means of the corresponding variables. The arrows indicate the respective contributions of different components involved in the water balance process. Error bars represent the 95% confidence interval.

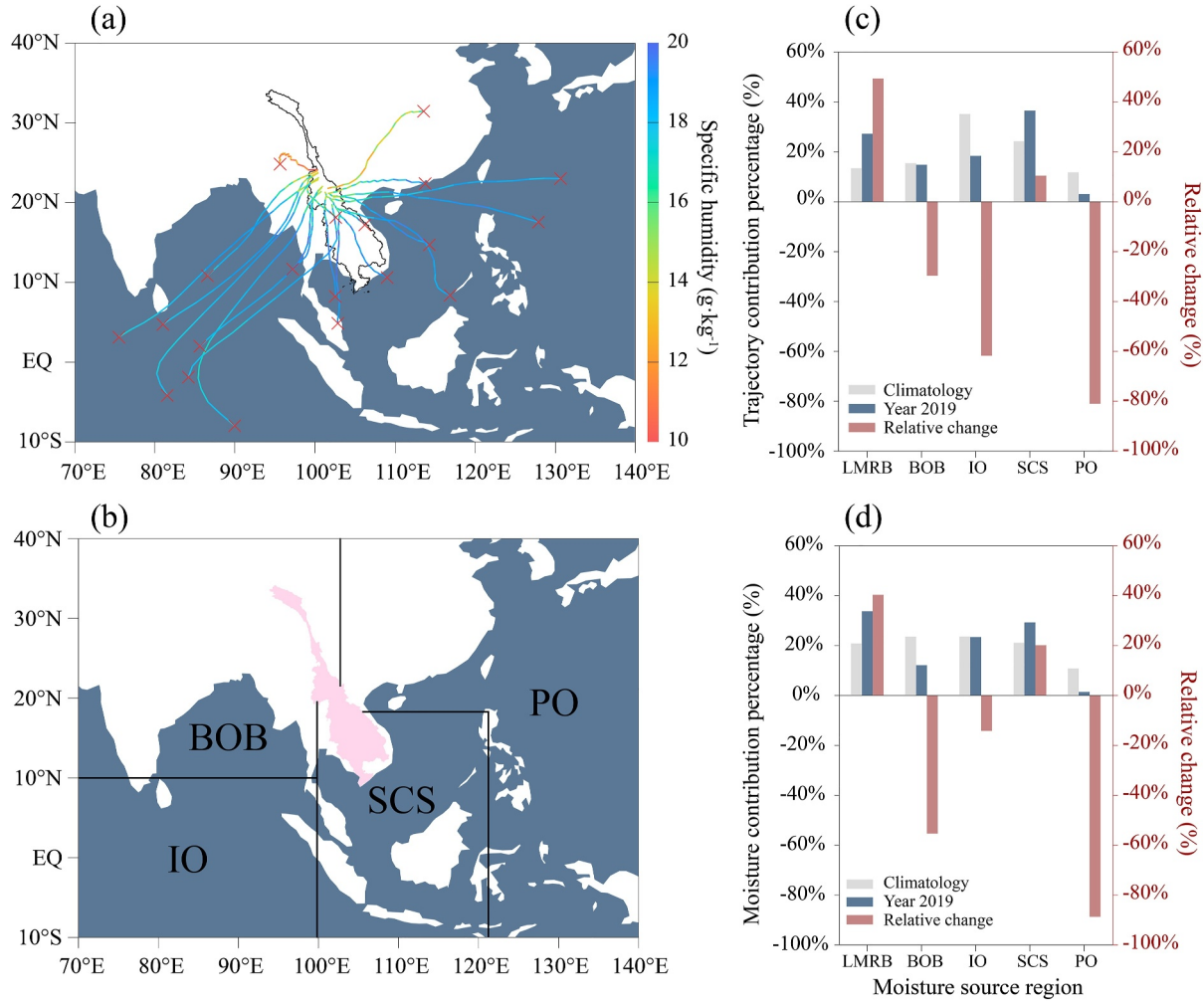

Figure 4. Moisture trajectories and contributions of trajectories from different regions. (a) Trajectories associated with precipitation in M-LMRB during the long-term mean of the wet season. Crosses in red indicate the moisture sources, while curves in color indicate the pathway of moisture transport trajectories; (b) These trajectory sources are organized into five groups: the pink area is the LMRB, and the other four regions are Bay of Bengal, Indian Ocean, Pacific Ocean and South China Sea; (c) contributions of the moisture transport pathways originated from the five regions in 2019 and the long-term means from May to October; (d) same as (c), but for moisture contribution.

evapotranspiration. The primary source of wet season precipitation in the M-LMRB was external water vapor, which accounted for 95.3% of the total precipitation, while local evapotranspiration contributed to the remaining source.

During the 2019 drought event, all grids show negative anomalies in precipitation minus evapotranspiration (base map). Compared to the long-term mean, there was only a minor decrease (1.2%) in evapotranspiration, while precipitation decreased significantly by 28.3%. The reduction in precipitation can be attributed to a combination of a 28.3% decline in external water vapor supply and a 23.6% decrease in internal water vapor supply. These declines jointly led to the 2019 surface runoff and soil water content being only 56.8% of the climatological average.

3.3. Moisture Sources and Pathways

A total of 312,984 trajectories associated with the moisture transport of M-LMRB during wet seasons of 1959–2021 were tracked using the HYSPLIT model. Among these, 87,062 trajectories contributed precipitation to the M-LMRB. Therefore, on average there have been 1,382 trajectories each year, but there were only 1,013 trajectories in 2019. These trajectories are clustered into 20 groups using SOM, as shown in Figure 4a. To

10.1029/2023EF004292

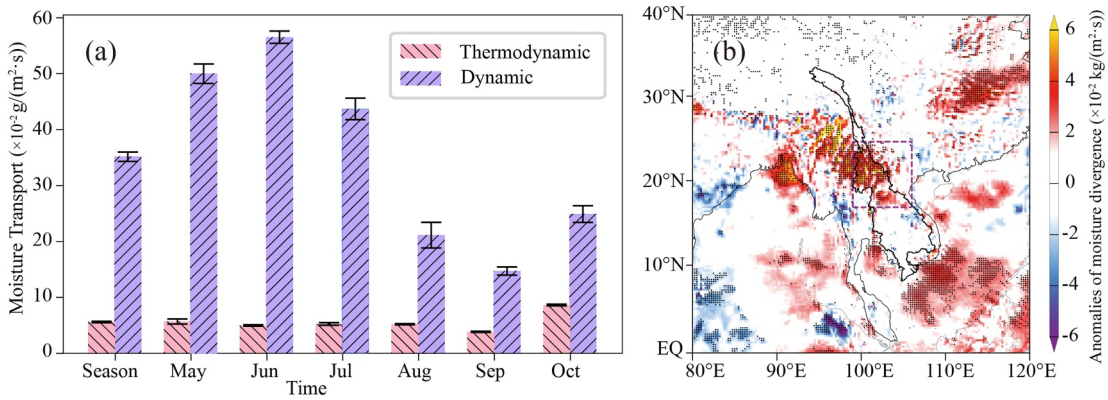

Figure 5. (a) Thermodynamic and dynamic components of the moisture transport in the M-LMRB during the 2019 wet season, Error bars represent the 95% confidence interval. (b) Vertically integrated water vapor flux divergence during the 2019 wet season, with stippling indicating anomalies significant at the 0.05 level.

quantitatively analyze the contributions of different moisture sources, these clusters are grouped into five regions according to the moisture sources: LMRB, Bay of Bengal (BOB), Indian Ocean (IO), South China Sea (SCS) and Pacific Ocean (PO), respectively (Figure 4b).

Among the different moisture sources, the pathway originating from the IO contributed the most to the total number of trajectories (35.2%) and total moisture (23.6%), as shown in Figures 4c and 4d. On the other hand, the pathway originating from the PO had the lowest contribution to the total number of trajectories (11.8%) and total moisture (10.8%). The remaining three regions (BOB, LMRB, and SCS) displayed similar moisture contributions to precipitation in the M-LMRB.

Pathways originating from the IO contributed the most to the total number of trajectories (35.2%) and the total moisture (23.6%) (Figures 4c and 4d). The pathways originating from the PO contributed the least to the total number of trajectories (11.8%) and total moisture (10.8%). The other three regions (BOB, LMRB, and SCS) had similar moisture contributions to the M-LMRB. Compared to the long-term mean, moisture sources originating from LMRB and SCS are found to have higher frequencies in both trajectories and moisture during this drought event. Specifically, the number of trajectories in the LMRB and SCS had increased from 185 to 335 (long-term mean) to 276 and 370 (2019), with 40.3% and 20.1% increase in moisture contribution, respectively. On the other hand, the two regions with the highest moisture contributions, IO and BOB, had negative anomalies in the number of tracks and moisture contributions, which had decreased from 486 to 213 (historical mean) to 186 and 150 (2019), respectively, and the moisture contribution had decreased by 14.1% and 55.4%, respectively. In addition, the most significant reductions in the number of trajectories (132) and moisture contributions (88.0%), are found in the Pacific Ocean (PO).

3.4. Dynamic and Thermodynamic Contribution of the 2019 Drought

The moisture transport associated with dynamics and thermodynamics processes, and vertically integrated water vapor flux divergence during the 2019 wet season were decomposed and shown in Figure 5. The thermodynamic component was about 5.6×10^{-2} g/(m^2·s) over M-LMRB, bringing moisture to the region by increasing specific humidity, while the dynamic component was 35.2×10^{-2} g/(m^2·s), which was 6.3 times that of the thermodynamic component. Specifically, there are disparities in the contributions of both components across different months. On one hand, the dynamical contribution varies notably across months, whereas the relative variation in the thermodynamic contribution remains relatively stable. On the other hand, periods with significant dynamical contributions are concentrated from May to July, with June being the peak month, contributing 56.5×10^{-2} g/(m^2·s), approximately 11.4 times that of the thermodynamic contribution during the same period. In addition, the vertically integrated water vapor flux divergence exhibited significant water vapor divergence over the M-LMRB (Figure 5c), indicating the dispersion or loss of water vapor from the region. These findings collectively indicate that the drought event in the M-LMRB during the 2019 wet season was primarily influenced by dynamic mechanisms rather than thermodynamic processes.

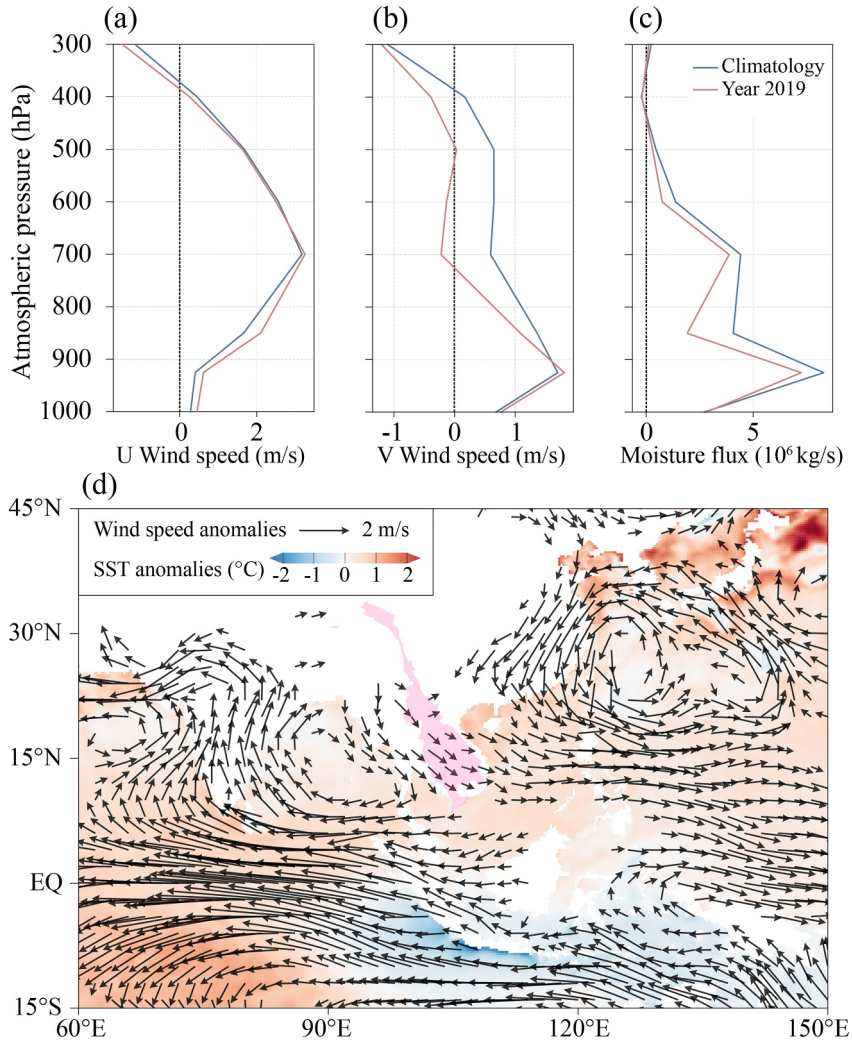

Figure 6. The atmospheric circulation background of the drought. (a) Zonal wind speed, (b) Meridional wind speed, and (c) $F_{in} - F_{out}$ at multiple pressure levels in the wet season of 2019 and the long-term mean; (d) the anomalies of wind field at 850 hPa in the 2019 wet season.

3.5. Atmospheric Circulation Background of the 2019 Drought

The U wind (zonal wind), V wind (meridional wind), and $F_{in} - F_{out}$ (inflow minus outflow of the atmospheric moisture) of the study area at multiple pressure levels during the wet season of 2019 and long-term means in the corresponding period are compared and presented in Figure 6. The results indicate that the U wind did not exhibit significant changes in 2019 compared to the long-term mean. However, the V wind showed a negative anomaly, particularly at 925–300 hPa, which was most significant with −0.8 m/s at an atmospheric pressure of 700 hPa, and the negative anomalies $F_{in} - F_{out}$ was most obvious at 850 hPa with a moisture flux reduction of 2.1 kg/s.

The anomalies in atmospheric circulation during the 2019 wet season were analyzed and presented in Figure 6d, revealing three key aspects:

1. The anomalous anticyclone formed over the Bay of Bengal: This anomalous anticyclone acted as a barrier, impeding the northward advancement of moisture-laden winds from the Indian Ocean toward Southeast Asia. As a result, the moisture transport toward the M-LMRB was hindered, contributing to a deficit in rainfall.
2. The Anomaly of easterly winds northeast of the Indian Ocean: In a typical scenario, the southwestern monsoon winds blow from the Indian Ocean toward Southeast Asia, bringing rainfall to the region. However, in 2019, an

unusual shift in the wind pattern occurred northeast of the Indian Ocean. This deviation disrupted the normal moisture transport, leading to a shortage of rainfall over the M-LMRB.

3. Anomaly of the western Pacific Ocean cyclone: East Asian summer wind-induced precipitation serves as a significant source of rainfall in Southeast Asia. However, anomalous anticyclones in the western Pacific Ocean hindered the transport of water vapor toward the M-LMRB. This disruption in moisture transport further exacerbated the drought conditions in the region.

4. Discussion and Conclusions

To explain the extreme drought event that occurred in M-LMRB in the 2019 wet season from the moisture transport aspect, the anomalies of water vapor circulation and transport in the M-LMRB were quantitatively analyzed in this study. The external and local moisture transport contributions in the wet seasons to the M-LMRB were estimated through a land-atmospheric water balance model. The HYSPLIT model and SOM were used to track the moisture transport pathways and cluster the trajectories, respectively. In addition, the contributions from thermodynamic and dynamic factors to anomalous moisture transport in the 2019 wet season of M-LMRB were quantified and compared.

Our analysis revealed that the majority of long-term precipitation in the study area, approximately 95.3%, was driven by external moisture sources, while a minor 4.7% contribution originated from local evapotranspiration. During the 2019 drought event, precipitation led by external advection decreased by 28.1%, while that by local evapotranspiration decreased by 23.6%. Consequently, surface runoff and soil moisture content were only 56.8% of the long-term mean during the corresponding period. According to the Mekong River Commission, the flow measured at stations in the Lower Mekong Basin in 2019 was approximately 53.8% of the long-term average (Mekong River Commission, 2022). This result falls between the calculated values of the PRR and those from ERA5, indicating a certain level of credibility in our findings. But how runoff is affected by external or internal moisture transport requires further discussion. Through the moisture transport trajectories, it was found that the precipitation of the study area is mainly from the Indian Ocean (IO), Bay of Bengal (BOB), and Pacific Ocean (PO). And during the drought in 2019, trajectories from these regions decreased by 14.2%, 55.4%, and 88.7%, respectively. Results obtained from decomposing the moisture transport into the dynamics and thermodynamics components indicate that dynamics-induced water vapor transport anomalies are about 6.3 times greater than thermodynamics, which means the atmospheric circulation, featuring the variation of the wind field, played a crucial role in the anomalous precipitation of this drought event.

By analyzing the anomalies of the vertical distribution of the wind field, the wind speed at 850 hPa was found to have significantly changed. The spatial distribution of the wind anomalies shows that the anomalous anticyclones formed over BOB and the anomalous cyclones over the western PO would facilitate the outflow of water vapor from the study area, leading to the occurrence of a prolonged drought in 2019. The India Meteorological Department reported a delay of 1 week in the arrival of the southwest monsoon, resulting in reduced precipitation in the LMRB during the early southwest monsoon season (Indian Meteorological Department, 2020). Explained spatially, atmospheric circulation anomalies in Southeast Asia are strongly related to sea surface temperature patterns. An extremely positive Indian Ocean Dipole (IOD) event took place in 2019, this event was characterized by cold sea surface temperature anomalies over the eastern equatorial Indian Ocean and warming in the western region. It had a significant impact on the direction of the southwestern monsoon winds from the Indian Ocean and led to weakened monsoon activity and reduced precipitation (Ratna et al., 2021). Furthermore, statistical analyses have shown a significant negative correlation between the PRR in the summer on the Tibetan Plateau and El Niño events occurring in the preceding winter. This correlation is associated with the presence of the anomalous Bengal Bay anticyclone (Zhao & Zhou, 2021). The occurrence of a weak El Niño event toward the end of 2018 may provide an explanation for the presence of the Bay of Bengal anticyclone observed in this study (Liu et al., 2020).

The 2016 drought event in the LMRB was considered the most severe apart from the 2019 event (Mekong River Commission, 2021), and its potential causes were quantitatively assessed. We evaluate the contribution of PRR (Figure S2 in Supporting Information S1) as well as thermodynamic and dynamic processes (Figure S3 in Supporting Information S1). Analysis shows that the drought in 2016 was mainly due to insufficient external water supply, while the contribution of local evapotranspiration increased compared with the same period in history. Similar to the 2019 findings, dynamic processes are still more influential than thermodynamic processes,

which is consistent with previous studies for the Asian monsoon region (Mahto et al., 2023; Sekizawa et al., 2019).

Observations over recent decades indicate a notable decrease in global land monsoon precipitation, particularly in the Northern Hemisphere, as summer monsoon precipitation shows a declining trend (M. H. Li et al., 2023; X. Li et al., 2023; Wang & Ding, 2006). Despite projections by multiple global climate models that South Asian monsoon precipitation would increase under ongoing global warming, it is expected that the duration of the summer monsoon may be shorter, resulting in lower overall precipitation (Sabeerali & Ajayamohan, 2018), climate model simulations indicate that the observed decrease in the regional monsoon precipitation during the second half of the 20th century is dominated by the radiative effects of Northern Hemisphere anthropogenic aerosols (Patil et al., 2019; Singh, 2016). Unlike the South Asian summer monsoon, the East Asian summer monsoon is expected to experience changes in location rather than intensity in response to global warming. These changes may lead to altered spatial patterns of floods and droughts (Li et al., 2010). Overall, the Asian monsoon region is projected to face more frequent drought events due to global climate change in the future (Ha et al., 2020).

This study encounters two limitations. While ideal PRR calculations typically demand flat terrain, the M-LMRB features significant altitude disparities, potentially increasing uncertainties. Second, previous research has not assessed the suitability of the HYSPLIT model-driven data set within the LMRB. Additionally, this study has yet to quantify the uncertainty in model output arising from disparate data sources. Further discourse and exploration are warranted in this aspect in the future.

Results from this study provide new insights into the understanding of the physical mechanisms of meteorological droughts in the mid-reaches of the Lancang-Mekong River Basin of wet to semi-wet climate. It is of great strategic significance to ensure water security, food security and ecological security of countries along the river basin.

Data Availability Statement

The ERA5 data used in this study can be found in Hersbach et al. (2020), the NCEP/NCAR-R1 data can be obtained from Kalnay et al. (2018), and the HYSPLIT software can be downloaded from Stein et al. (2015).

Acknowledgments
This work was supported by the National Natural Science Foundation of China (Grant 42361144001) and the Henan Provincial Key Laboratory of Hydrosphere and Watershed Water Security. The Guangdong Basic and Applied Basic Research Foundation (Grant 2022A1515011070) are also acknowledged for partially financing this work.

References

Ault, T. R. (2020). On the essentials of drought in a changing climate. *Science*, *368*(6488), 256–260. https://doi.org/10.1126/science.aaz5492

Barichivich, J., Gloor, E., Peylin, P., Brienen, R. J., Schöngart, J., Espinoza, J. C., & Pattnayak, K. C. (2018). Recent intensification of Amazon flooding extremes driven by strengthened Walker circulation. *Science Advances*, *4*(9), eaat8785. https://doi.org/10.1126/sciadv.aat8785

Bevacqua, E., Zappa, G., Lehner, F., & Zscheischler, J. (2022). Precipitation trends determine future occurrences of compound hot-dry events. *Nature Climate Change*, *12*(4), 350–355. https://doi.org/10.1038/s41558-022-01309-5

Brás, T. A., Seixas, J., Carvalhais, N., & Jägermeyr, J. (2021). Severity of drought and heatwave crop losses tripled over the last five decades in Europe. *Environmental Research Letters*, *16*(6), 065012. https://doi.org/10.1088/1748-9326/abf004

Brubaker, K. L., Entekhabi, D., & Eagleson, P. S. (1993). Estimation of continental precipitation recycling. *Journal of Climate*, *6*(6), 1077–1089. https://doi.org/10.1175/1520-0442(1993)006<1077:EOCPR>2.0.CO;2

Burde, G. I., & Zangvil, A. (2001). The estimation of regional precipitation recycling. Part I: Review of recycling models. *Journal of Climate*, *14*(12), 2497–2508. https://doi.org/10.1175/1520-0442(2001)014<2497:TEORPR>2.0.CO;2

Burls, N. J., Blamey, R. C., Cash, B. A., Swenson, E. T., Fahad, A. A., Bopape, M. J. M., et al. (2019). The Cape Town "day zero" drought and Hadley cell expansion. *Npj Climate and Atmospheric Science*, *2*(1), 27. https://doi.org/10.1038/s41612-019-0084-6

Chang, F. J., Chang, L. C., Kao, H. S., & Wu, G. R. (2010). Assessing the effort of meteorological variables for evaporation estimation by self-organizing map neural network. *Journal of Hydrology*, *384*(1–2), 118–129. https://doi.org/10.1016/j.jhydrol.2010.01.016

Chiang, F., Mazdiyasni, O., & AghaKouchak, A. (2021). Evidence of anthropogenic impacts on global drought frequency, duration, and intensity. *Nature Communications*, *12*(1), 2754. https://doi.org/10.1038/s41467-021-22314-w

Daniel, T., Patrick, A., & Huang, Z. (2022). DROUGHT IN NUMBERS 2022 restoration for readiness and resilience (p. 37).

de Medeiros, F. J., de Oliveira, C. P., Santos e Silva, C. M., & de Araújo, J. M. (2020). Numerical simulation of the circulation and tropical teleconnection mechanisms of a severe drought event (2012–2016) in Northeastern Brazil. *Climate Dynamics*, *54*(9–10), 4043–4057. https://doi.org/10.1007/s00382-020-05213-6

Dey, D., & Döös, K. (2020). Atmospheric freshwater transport from the Atlantic to the Pacific Ocean: A Lagrangian analysis. *Geophysical Research Letters*, *47*(6), e2019GL086176. https://doi.org/10.1029/2019GL086176

Diekmann, C. J., Schneider, M., Knippertz, P., de Vries, A. J., Pfahl, S., Aemisegger, F., et al. (2021). A Lagrangian perspective on stable water isotopes during the West African Monsoon. *Journal of Geophysical Research: Atmospheres*, *126*(19), e2021JD034895. https://doi.org/10.1029/2021JD034895

Dong, Z., Liu, H., Hu, H., Khan, M. Y. A., Wen, J., Chen, L., & Tian, F. (2022). Future projection of seasonal drought characteristics using CMIP6 in the Lancang-Mekong River Basin. *Journal of Hydrology*, *610*, 127815. https://doi.org/10.1016/j.jhydrol.2022.127815

Draxler, R. R., & Hess, G. D. (1998). An overview of the HYSPLIT_4 modelling system for trajectories. *Australian Meteorological Magazine*, *47*(4), 295–308.

Eltahir, E. A., & Bras, R. L. (1994). Precipitation recycling in the Amazon basin. *Quarterly Journal of the Royal Meteorological Society*, *120*(518), 861–880. https://doi.org/10.1002/qj.49712051806

Eltahir, E. A., & Bras, R. L. (1996). Precipitation recycling. *Reviews of Geophysics*, *34*(3), 367–378. https://doi.org/10.1029/96RG01927

Feng, Y., Wang, W., Suman, D., Yu, S., & He, D. (2019). Water cooperation priorities in the Lancang-Mekong River basin based on cooperative events since the Mekong River Commission establishment. *Chinese Geographical Science*, *29*(1), 58–69. https://doi.org/10.1007/s11769-019-1016-4

Gu, L., Chen, J., Yin, J., Xu, C. Y., & Zhou, J. (2020). Responses of precipitation and runoff to climate warming and implications for future drought changes in China. *Earth's Future*, *8*(10), e2020EF001718. https://doi.org/10.1029/2020EF001718

Gualtieri, G. (2022). Analysing the uncertainties of reanalysis data used for wind resource assessment: A critical review. *Renewable and Sustainable Energy Reviews*, *167*, 112741. https://doi.org/10.1016/j.rser.2022.112741

Guan, Y., Gu, X., Slater, L. J., Li, L., Kong, D., Liu, J., et al. (2022). Tracing anomalies in moisture recycling and transport to two record-breaking droughts over the Mid-to-Lower Reaches of the Yangtze River. *Journal of Hydrology*, *609*, 127787. https://doi.org/10.1016/j.jhydrol.2022.127787

Guntu, R. K., Maheswaran, R., Agarwal, A., & Singh, V. P. (2020). Accounting for temporal variability for improved precipitation regionalization based on self-organizing map coupled with information theory. *Journal of Hydrology*, *590*, 125236. https://doi.org/10.1016/j.jhydrol.2020.125236

Guo, X., Tian, L., Wang, L., Wang, Y., & Zhou, J. (2023). Controls of the recent precipitation anomalies in the southeastern Tibetan Plateau: From the perspective of Indian summer monsoon activities and moisture sources. *Climate Dynamics*, *62*, 1–14. https://doi.org/10.1007/s00382-023-06919-z

Gupta, A., Hock, L., Xiaojing, H., & Ping, C. (2002). Evaluation of part of the Mekong River using satellite imagery. *Geomorphology*, *44*(3–4), 221–239. https://doi.org/10.1016/S0169555X(01)00176-3

Ha, K. J., Moon, S., Timmermann, A., & Kim, D. (2020). Future changes of summer monsoon characteristics and evaporative demand over Asia in CMIP6 simulations. *Geophysical Research Letters*, *47*(8), e2020GL087492. https://doi.org/10.1029/2020GL087492

Hersbach, H., Bell, B., Berrisford, P., Hirahara, S., Horányi, A., Muñoz-Sabater, J., et al. (2020). The ERA5 global reanalysis [Dataset]. ERA5. *Quarterly Journal of the Royal Meteorological Society*, *146*(730), 1999–2049. https://doi.org/10.1002/qj.3803

Horton, D. E., Johnson, N. C., Singh, D., Swain, D. L., Rajaratnam, B., & Diffenbaugh, N. S. (2015). Contribution of changes in atmospheric circulation patterns to extreme temperature trends. *Nature*, *522*(7557), 465–469. https://doi.org/10.1038/nature14550

Indian Meteorological Department. (2020). 2019 southwest monsoon end of season report (p. 2).

Irannezhad, M., Liu, J., & Chen, D. (2020). Influential climate teleconnections for spatiotemporal precipitation variability in the Lancang-Mekong River basin from 1952 to 2015. *Journal of Geophysical Research: Atmospheres*, *125*(21), e2020JD033331. https://doi.org/10.1029/2020JD033331

Irannezhad, M., Liu, J., & Chen, D. (2022). Extreme precipitation variability across the Lancang-Mekong River Basin during 1952–2015 in relation to teleconnections and summer monsoons. *International Journal of Climatology*, *42*(5), 2614–2638. https://doi.org/10.1002/joc.7370

Jing, W., Zhao, X., Yao, L., Jiang, H., Xu, J., Yang, J., & Li, Y. (2020). Variations in terrestrial water storage in the Lancang-Mekong river basin from GRACE solutions and land surface model. *Journal of Hydrology*, *580*, 124258. https://doi.org/10.1016/j.jhydrol.2019.124258

Kalnay, E., Kanamitsu, M., Kistler, R., Collins, W., Deaven, D., Gandin, L., et al. (2018). The NCEP/NCAR 40-year reanalysis project [Dataset]. *NCEP/NCAR-R1. Renewable Energy*, Vol1_146–Vol1_194. https://doi.org/10.1175/1520-0477(1996)077<0437:TNYRP>2.0.CO;2

Kumari, A., Kumar, P., Dubey, A. K., Mishra, A. K., & Saharwardi, M. S. (2022). Dynamical and thermodynamical aspects of precipitation events over India. *International Journal of Climatology*, *42*(5), 3094–3106. https://doi.org/10.1002/joc.7409

Li, J., Wu, Z., Jiang, Z., & He, J. (2010). Can global warming strengthen the East Asian summer monsoon? *Journal of Climate*, *23*(24), 6696–6705. https://doi.org/10.1175/2010JCLI3434.1

Li, M. H., Vu, T. M., & Chen, P. Y. (2023). Multiple drought indices and their teleconnections with ENSO in various spatiotemporal scales over the Mekong River Basin. *Science of the Total Environment*, *854*, 158589. https://doi.org/10.1016/j.scitotenv.2022.158589

Li, X., Wang, L., Chen, D., Thompson, L., Yang, K., Zhong, S., et al. (2023). Large-scale circulation dominated precipitation variation and its effect on potential water availability across the Tibetan Plateau. *Environmental Research Letters*, *18*(7), 074018. https://doi.org/10.1088/1748-9326/acdd15

Li, Z., Smerdon, J. E., Seager, R., Siegert, N., & Mankin, J. S. (2024). Emergent trends complicate the interpretation of the United States Drought Monitor (USDM). *AGU Advances*, *5*(2), e2023AV001070. https://doi.org/10.1029/2023av001070

Liao, Z., Xie, J., Fang, X., Wang, Y., Zhang, Y., Xu, X., & Fan, S. (2020). Modulation of synoptic circulation to dry season PM2. 5 pollution over the Pearl River Delta region: An investigation based on self-organizing maps. *Atmospheric Environment*, *230*, 117482. https://doi.org/10.1016/j.atmosenv.2020.117482

Liu, J., Chen, D., Mao, G., Irannezhad, M., & Pokhrel, Y. (2022). Past and future changes in climate and water resources in the Lancang–Mekong River Basin: Current understanding and future research directions. *Engineering*, *13*, 144–152. https://doi.org/10.1016/j.eng.2021.06.026

Liu, X., Yang, M., Wang, H., Liu, K., Dong, N., Wang, H., et al. (2023). Moisture sources and atmospheric circulation associated with the record-breaking rainstorm over Zhengzhou city in July 2021. *Natural Hazards*, *116*(1), 817–836. https://doi.org/10.1007/s11069-022-05700-5

Liu, Y., Hu, Z. Z., & Wu, R. (2020). Was the extremely wet winter of 2018/2019 in the lower reach of the Yangtze River driven by El Niño–Southern Oscillation? *International Journal of Climatology*, *40*(15), 6441–6457. https://doi.org/10.1002/joc.6591

Loikith, P. C., Lintner, B. R., & Sweeney, A. (2017). Characterizing large-scale meteorological patterns and associated temperature and precipitation extremes over the northwestern United States using self-organizing maps. *Journal of Climate*, *30*(8), 2829–2847. https://doi.org/10.1175/JCLI-D-16-0670.1

Lu, X. X., & Chua, S. D. X. (2021). River discharge and water level changes in the Mekong River: Droughts in an era of mega-dams. *Hydrological Processes*, *35*(7), e14265. https://doi.org/10.1002/hyp.14265

Lu, Y., Tian, F., Guo, L., Borzì, I., Patil, R., Wei, J., et al. (2021). Socio-hydrologic modeling of the dynamics of cooperation in the transboundary Lancang–Mekong River. *Hydrology and Earth System Sciences*, *25*(4), 1883–1903. https://doi.org/10.5194/hess-25-1883-2021

Mahto, S. S., & Mishra, V. (2019). Does ERA-5 outperform other reanalysis products for hydrologic applications in India? *Journal of Geophysical Research: Atmospheres*, *124*(16), 9423–9441. https://doi.org/10.1029/2019jd031155

Mahto, S. S., Nayak, M. A., Lettenmaier, D. P., & Mishra, V. (2023). Atmospheric rivers that make landfall in India are associated with flooding. *Communications Earth & Environment*, *4*(1), 120. https://doi.org/10.1038/s43247-023-00775-9

Marengo, J. A., Alves, L. M., Alvala, R., Cunha, A. P., Brito, S., & Moraes, O. L. (2017). Climatic characteristics of the 2010-2016 drought in the semiarid Northeast Brazil region. *Anais da Academia Brasileira de Ciências*, *90*(2 suppl 1), 1973–1985. https://doi.org/10.1590/0001-3765201720170206

Markonis, Y., Kumar, R., Hanel, M., Rakovec, O., Máca, P., & AghaKouchak, A. (2021). The rise of compound warm-season droughts in Europe. *Science Advances*, *7*(6), eabb9668. https://doi.org/10.1126/sciadv.abb9668

Mekong River Commission. (2021). Annual Mekong hydrology, flood and drought report 2019: Drought in the lower Mekong Basin.

Mekong River Commission. (2022). Mekong low flow and drought conditions in 2019-2021: Hydrological conditions in the lower Mekong River Basin. *Mekong River Commission: Vientiane, Laos*.

Nguyen, H., & Shaw, R. (2011a). Chapter 3 adaptation to droughts in Cambodia. In *Droughts in Asian monsoon region* (pp. 49–66). Emerald Group Publishing Limited. https://doi.org/10.1108/S2040-7262(2011)0000008009

Nguyen, H., & Shaw, R. (2011b). Chapter 8 drought risk management in Vietnam. In *Droughts in Asian monsoon region* (pp. 141–161). Emerald Group Publishing Limited. https://doi.org/10.1108/S2040-7262(2011)8

Nogueira, M. (2020). Inter-comparison of ERA-5, ERA-interim and GPCP rainfall over the last 40 years: Process-based analysis of systematic and random differences. *Journal of Hydrology*, *583*, 124632. https://doi.org/10.1016/j.jhydrol.2020.124632

Olauson, J. (2018). ERA5: The new champion of wind power modelling? *Renewable Energy*, *126*, 322–331. https://doi.org/10.1016/j.renene.2018.03.056

Parmesan, C., Morecroft, M. D., & Trisurat, Y. (2022). Climate change 2022: Impacts, adaptation and vulnerability (Doctoral dissertation, GIEC). https://doi.org/10.1017/9781009325844

Patil, N., Venkataraman, C., Muduchuru, K., Ghosh, S., & Mondal, A. (2019). Disentangling sea-surface temperature and anthropogenic aerosol influences on recent trends in South Asian monsoon rainfall. *Climate Dynamics*, *52*(3–4), 2287–2302. https://doi.org/10.1007/s00382-018-4251-y

Phan-Van, T., Nguyen-Ngoc-Bich, P., Ngo-Duc, T., Vu-Minh, T., Le, P. V., Trinh-Tuan, L., et al. (2022). Drought over Southeast Asia and its association with large-scale drivers. *Journal of Climate*, *35*(15), 4959–4978. https://doi.org/10.1175/JCLI-D-21-0770.1

Ratna, S. B., Cherchi, A., Osborn, T. J., Joshi, M., & Uppara, U. (2021). The extreme positive Indian Ocean dipole of 2019 and associated Indian summer monsoon rainfall response. *Geophysical Research Letters*, *48*(2), e2020GL091497. https://doi.org/10.1029/2020GL091497

Sabeerali, C. T., & Ajayamohan, R. S. (2018). On the shortening of Indian summer monsoon season in a warming scenario. *Climate Dynamics*, *50*(5–6), 1609–1624. https://doi.org/10.1007/s00382-017-3709-7

Sam, T. T., Khoi, D. N., Thao, N. T. T., Nhi, P. T. T., Quan, N. T., Hoan, N. X., & Nguyen, V. T. (2019). Impact of climate change on meteorological, hydrological and agricultural droughts in the lower Mekong River Basin: A case study of the Srepok Basin, Vietnam. *Water and Environment Journal*, *33*(4), 547–559. https://doi.org/10.1111/wej.12424

Seager, R., Naik, N., & Vecchi, G. A. (2010). Thermodynamic and dynamic mechanisms for large-scale changes in the hydrological cycle in response to global warming. *Journal of Climate*, *23*(17), 4651–4668. https://doi.org/10.1175/2010JCLI3655.1

Sekizawa, S., Miyasaka, T., Nakamura, H., Shimpo, A., Takemura, K., & Maeda, S. (2019). Anomalous moisture transport and oceanic evaporation during a torrential rainfall event over western Japan in early July 2018. *SOLA*, *15A-005*(0), 25–30. https://doi.org/10.2151/sola.15A-005

Shah, D., & Mishra, V. (2020). Drought onset and termination in India. *Journal of Geophysical Research: Atmospheres*, *125*(15), e2020JD032871. https://doi.org/10.1029/2020JD032871

Shi, Y., Jiang, Z., Liu, Z., & Li, L. (2020). A Lagrangian analysis of water vapor sources and pathways for precipitation in East China in different stages of the East Asian summer monsoon. *Journal of Climate*, *33*(3), 977–992. https://doi.org/10.1175/JCLI-D-19-0089.1

Singh, D. (2016). Tug of war on rainfall changes. *Nature Climate Change*, *6*(1), 20–22. https://doi.org/10.1038/nclimate2901

Sodemann, H., Schwierz, C., & Wernli, H. (2008). Interannual variability of Greenland winter precipitation sources: Lagrangian moisture diagnostic and North Atlantic Oscillation influence. *Journal of Geophysical Research*, *113*(D3), D03107. https://doi.org/10.1029/2007JD008503

Spassiani, A. C., & Mason, M. S. (2021). Application of Self-organizing Maps to classify the meteorological origin of wind gusts in Australia. *Journal of Wind Engineering and Industrial Aerodynamics*, *210*, 104529. https://doi.org/10.1016/j.jweia.2021.104529

Stein, A. F., Draxler, R. R., Rolph, G. D., Stunder, B. J., Cohen, M. D., & Ngan, F. (2015). NOAA's HYSPLIT atmospheric transport and dispersion modeling system (Version 5.1.0) [Software]. *HYSPLIT. Bulletin of the American Meteorological Society*, *96*(12), 2059–2077. https://doi.org/10.1175/BAMS-D-14-00110.1

Sui, C. H., Li, X., & Yang, M. J. (2007). On the definition of precipitation efficiency. *Journal of the Atmospheric Sciences*, *64*(12), 4506–4513. https://doi.org/10.1175/2007JAS2332.1

Sun, D. Z., & Lindzen, R. S. (1993). Distribution of tropical tropospheric water vapor. *Journal of the Atmospheric Sciences*, *50*(12), 1643–1660. https://doi.org/10.1175/1520-0469(1993)050<1643:DOTTWV>2.0.CO;2

Suthinkumar, P. S., Varikoden, H., & Babu, C. A. (2023). Changes in extreme rainfall events in the recent decades and their linkage with atmospheric moisture transport. *Global and Planetary Change*, *221*, 104047. https://doi.org/10.1016/j.gloplacha.2023.104047

Tan, X., Chen, S., Gan, T. Y., Liu, B., & Chen, X. (2019). Dynamic and thermodynamic changes conducive to the increased occurrence of extreme spring fire weather over western Canada under possible anthropogenic climate change. *Agricultural and Forest Meteorology*, *265*, 269–279. https://doi.org/10.1016/j.agrformet.2018.11.026

Tang, X., Woodcock, C. E., Olofsson, P., & Hutyra, L. R. (2021). Spatiotemporal assessment of land use/land cover change and associated carbon emissions and uptake in the Mekong River Basin. *Remote Sensing of Environment*, *256*, 112336. https://doi.org/10.1016/j.rse.2021.112336

Tian, F., Liu, H., Hou, S., Li, K., Lu, H., Ni, G., et al. (2020). *Drought characteristics of Lancang-Mekong River Basin and the impacts of reservoir regulation on streamflow. Centre for International Transboundary Water and Eco-Security, Tsinghua University and Department of Hydraulics*. China Institute of Water Resources and Hydropower Research.

Tian, L., Zhang, B., Chen, S., Wang, X., Ma, X., & Pan, B. (2022). Large-scale afforestation enhances precipitation by intensifying the atmospheric water cycle over the Chinese Loess Plateau. *Journal of Geophysical Research: Atmospheres*, *127*(16), e2022JD036738. https://doi.org/10.1029/2022JD036738

van der Wiel, K., Batelaan, T. J., & Wanders, N. (2023). Large increases of multi-year droughts in north-western Europe in a warmer climate. *Climate Dynamics*, *60*(5–6), 1781–1800. https://doi.org/10.1007/s00382-022-06373-3

Wang, B., & Ding, Q. (2006). Changes in global monsoon precipitation over the past 56 years. *Geophysical Research Letters*, *33*(6), L06711. https://doi.org/10.1029/2005GL025347

Wang, C., Chen, J., Gu, L., Wu, G., Tong, S., Xiong, L., & Xu, C. Y. (2023). A pathway analysis method for quantifying the contributions of precipitation and potential evapotranspiration anomalies to soil moisture drought. *Journal of Hydrology*, *621*, 129570. https://doi.org/10.1016/j.jhydrol.2023.129570

Wang, G., Cai, W., Yang, K., Santoso, A., & Yamagata, T. (2020). A unique feature of the 2019 extreme positive Indian Ocean Dipole event. *Geophysical Research Letters*, *47*(18), e2020GL088615. https://doi.org/10.1029/2020GL088615

Wang, J., Tang, Q., Chen, A., Tang, Y., Xu, X., Yun, X., et al. (2022). Impacts of summer monsoons on flood characteristics in the Lancang-Mekong River Basin. *Journal of Hydrology*, *604*, 127256. https://doi.org/10.1016/j.jhydrol.2021.127256

Wang, T., Zhao, Y., Xu, C., Ciais, P., Liu, D., Yang, H., et al. (2021). Atmospheric dynamic constraints on Tibetan Plateau freshwater under Paris climate targets. *Nature Climate Change*, *11*(3), 219–225. https://doi.org/10.1038/s41558-020-00974-8

Xiong, J., Guo, S., Chen, J., & Yin, J. (2022). A reexamination of the dry gets drier and wet gets wetter paradigm over global land: Insight from terrestrial water storage changes. *Hydrology and Earth System Sciences Discussions*, 1–20. https://doi.org/10.5194/hess-2022-190

Yang, T., Ding, J., Liu, D., Wang, X., & Wang, T. (2019). Combined use of multiple drought indices for global assessment of dry gets drier and wet gets wetter paradigm. *Journal of Climate*, *32*(3), 737–748. https://doi.org/10.1175/JCLI-D-18-0261.1

Yuan, Y., Du, T., Wang, H., & Wang, L. (2020). Novel Keeling-plot-based methods to estimate the isotopic composition of ambient water vapor. *Hydrology and Earth System Sciences*, *24*(9), 4491–4501. https://doi.org/10.5194/hess-24-4491-2020

Yun, X., Tang, Q., Sun, S., & Wang, J. (2021). Reducing climate change induced flood at the cost of hydropower in the Lancang-Mekong River Basin. *Geophysical Research Letters*, *48*(20), e2021GL094243. https://doi.org/10.1029/2021GL094243

Zhang, S., Zhang, G., Gong, G., Gan, T. Y., Chen, D., & Liu, J. (2024). Moisture sources and pathways of annual maximum precipitation in the Lancang-Mekong River Basin. *Geophysical Research Letters*, *51*(6), e2023GL107622. https://doi.org/10.1029/2023GL107622

Zhao, Y., & Zhou, T. (2021). Interannual variability of precipitation recycle ratio over the Tibetan Plateau. *Journal of Geophysical Research: Atmospheres*, *126*(2), e2020JD033733. https://doi.org/10.1029/2020JD033733